

Title

Differential transgene silencing of myeloid-specific promoters in the *AAVS1* safe harbor locus of iPSC-derived myeloid cells

Authors

Denise Klatt^{1,2}, Erica Cheng^{1,2}, Dirk Hoffmann^{1,2}, Giorgia Santilli³, Adrian J Thrasher^{3,4},
Christian Brendel⁵, Axel Schambach^{1,2,6}

Affiliations

¹ Institute of Experimental Hematology, Hannover Medical School, 30625 Hannover, Germany

² REBIRTH Cluster of Excellence, Hannover Medical School, 30625 Hannover, Germany

³ Infection, Immunity and Inflammation Program, Molecular and Cellular Immunology Section, UCL Great Ormond Street Institute of Child Health, University College London, London WC1N 1EH, UK

⁴ Great Ormond Street Hospital NHS Foundation Trust, London WC1N 1EH, UK

⁵ Dana-Farber/Boston Children's Cancer and Blood Disorders Center, Harvard Medical School, Boston, MA 02115, USA

⁶ Division of Hematology/Oncology, Boston Children's Hospital, Harvard Medical School, Boston, MA 02115, USA

Corresponding author

Prof. Dr. med. Axel Schambach, PhD

Institute of Experimental Hematology

Hannover Medical School

Carl-Neuberg-Str.1

D-30625 Hannover

Phone: +49 511-532-6067

Email: schambach.axel@mh-hannover.de

Short title

Differential transgene silencing in the *AAVS1* site

Abstract

Targeted integration into a genomic safe harbor, such as the *AAVS1* locus on chromosome 19, promises predictable transgene expression and reduces the risk of insertional mutagenesis in the host genome. The application of gamma-retroviral LTR-driven vectors, which semi-randomly integrate into the genome, has previously caused severe adverse events in some clinical studies due to transactivation of neighboring proto-oncogenes. Consequently, the site-specific integration of a therapeutic transgene into a genomic safe harbor locus would allow stable genetic correction with a reduced risk of insertional mutagenesis. However, recent studies revealed that transgene silencing, especially in case of weaker cell type-specific promoters, can occur in the *AAVS1* locus of human pluripotent stem cells (PSC) and can impede transgene expression during differentiation. In this study, we aimed to correct $p47^{\text{phox}}$ -deficiency, which is the second most common cause of chronic granulomatous disease, by insertion of a therapeutic $p47^{\text{phox}}$ transgene into the *AAVS1* locus of human induced PSC (iPSC) using CRISPR-Cas9. We analyzed transgene expression and functional correction from three different myeloid-specific promoters (miR223, CatG/cFes and MRP8). Upon myeloid differentiation of corrected iPSC clones, we observed that the miR223 and CatG/cFes promoter achieved therapeutic-relevant levels of $p47^{\text{phox}}$ expression and NADPH oxidase activity, whereas the MRP8 promoter was less efficient. Analysis of the different promoters revealed high CpG methylation of the MRP8 promoter in differentiated cells, which correlated with the transgene expression data. In summary, we identified the miR223 and CatG/cFes promoters as cell type-specific promoters that allow stable transgene expression in the *AAVS1* locus of iPSC-derived myeloid cells. Our findings further indicate that promoter silencing can occur in the *AAVS1* safe harbor locus in differentiated hematopoietic cells and that a comparison of different promoters is necessary to achieve optimal transgene expression for therapeutic application of iPSC-derived cells.

Introduction

The discovery of the CRISPR-Cas9 system and its development as a gene editing tool has accelerated and broadened the application of designer nucleases to study gene functions in basic biology or to treat genetic diseases in clinical trials¹. Designer nucleases allow site-specific correction of a point mutation or insertion of a therapeutic minigene. These strategies reduce the risk of insertional mutagenesis, which has been observed in the past using LTR-driven gamma-retroviral vectors for gene therapy²⁻⁶. In these studies, gamma-retroviral vectors semi-randomly integrated into the host genome and caused transactivation of adjacent proto-oncogenes, which caused acute leukemia in some cases. In contrast to retroviral vectors, a gene correction approach that directly targets the mutated gene or a safe harbor locus, e.g. the *AAVS1* locus or the *CCR5* gene, could avoid insertional mutagenesis as well as unpredictable transgene silencing, which has also been observed for retroviral vectors^{7,8}. A genomic safe harbor locus is defined by two major criteria: (I) the inserted gene expression cassette functions predictably and (II) it does not alter the host genome by means of gene disruption or activation of neighboring genes^{7,9}. Another advantage of targeting a safe harbor locus for gene therapy is that the complete cDNA is inserted into the patient genome, so that the same correction strategy could be applied for all patients independent of their underlying disease-causing mutation. In contrast, approaches that directly target the mutated gene may require development of specific strategies for different mutations, including a costly and time consuming detailed risk evaluation for each approach. However, similar to a retroviral gene addition approach, a tailored and optionally lineage/tissue-specific promoter to drive cell type-specific expression of the transgene is also needed in a genomic safe harbor locus. Although many compact cell type-specific promoters have been developed in the past years and are already clinically used in gene therapy trials, they do not completely recapitulate the endogenous promoter in terms of spatiotemporal expression and could be epigenetically silenced in human induced pluripotent stem cells (iPSC) during lineage-specific differentiation. In addition to their potential to differentiate into cells of almost all lineages, iPSC provide an unlimited autologous stem cell source for future cell therapies. Moreover, iPSC can be generated via reprogramming patient-derived somatic cells and can

be used as models to study disease pathophysiology and to develop novel gene and cell therapies.

In this study, we used CRISPR-Cas9 to correct p47^{phox} deficiency, an autosomal-recessive form of chronic granulomatous disease (CGD), which is caused by mutations of the p47^{phox} subunit of the nicotinamide adenine dinucleotide (NADPH) oxidase. The NADPH oxidase is found in the membrane of phagosomes in phagocytic cells, where it transfers electrons from NADPH to molecular O₂ to generate superoxide anions and other reactive oxygen species (ROS) upon stimulation, e.g. the phagocytosis of microbes¹⁰⁻¹². ROS generation results in a change of the phagosome milieu, which leads to the release of different granules into the phagosome. These granules contain antimicrobial proteins, e.g. myeloperoxidase and defensins, which synergize with the produced ROS to mediate killing of the encountered microbes. Due to the lack of NADPH oxidase activity, CGD patients suffer from severe bacterial and fungal infections and the formation of granulomas in various organs, which can be life-threatening¹³. Only hematopoietic stem cell (HSC) transplantation and potentially gene therapy are curative treatment options. The p47^{phox}-subunit is encoded by *NCF1*, which has two highly homologous pseudogenes *NCF1B* and *NCF1C* on the same chromosome¹⁴⁻¹⁸. Over 90% of p47-CGD patients share the same disease-causing mutation, namely the dinucleotide deletion c.75_76delGT (Δ GT) in exon 2¹⁹. This Δ GT mutation is also found in the two pseudogenes of healthy individuals. It is hypothesized that the Δ GT mutation is copied into the functional *NCF1* gene from one of the two pseudogenes via gene conversion and consequently causes the disease¹⁸. Merling *et al.* demonstrated the feasibility of a gene editing approach to directly correct the Δ GT mutation in patient-derived p47^{phox}-deficient iPSC²⁰. They showed that even the correction of the Δ GT mutation in the pseudogenes can restore p47^{phox} expression. However, in a gene editing approach the presence of the two pseudogenes could be problematic because of multiple DSB that are introduced into the genome due to the sequence homology between *NCF1* and its pseudogene. The introduction of multiple DSB increases the risk of unwanted off-target effects, e.g. larger deletions or inversions. Moreover, the pseudogenes could compete with the therapeutic donor template for HDR and could reintroduce the false sequence into the host genome, which could potentially reduce the overall gene editing efficiency.

To avoid potential difficulties with gene editing in the *NCF1* locus, we targeted the *AAVS1* safe harbor locus on chromosome 19 to correct $p47^{\text{phox}}$ -deficiency. Recently, Ordovàs *et al.* demonstrated that the *AAVS1* locus is not as “safe” as previously thought to be²¹. The authors observed transgene silencing of different cell type-specific promoters that were inserted into the *AAVS1* locus in embryonic stem cells and differentiated hepatocytes. As $p47^{\text{phox}}$ expression is restricted to the myeloid lineage, we tested three different myeloid-specific promoters (the miR223 promoter²², the chimeric *CathepsinG* and *cFes* (CatG/cFes)²³ promoter and the myeloid-related protein 8 (MRP8) promoter²⁴) and analyzed which promoter provided reliable transgene expression in the *AAVS1* locus of differentiated iPSC. Upon myeloid differentiation of corrected iPSC, we observed that the miR223 and CatG/cFes promoters yielded similar or slightly lower $p47^{\text{phox}}$ expression levels and NADPH oxidase activity as wild type cells. In contrast, we observed increased DNA methylation of the MRP8 promoter compared to the miR223 and CatG/cFes promoters in differentiated cells, which correlated with the reduced expression from the MRP8 promoter. In summary, we demonstrated that the myeloid-specific miR223 and CatG/cFes promoters allow stable transgene expression in iPSC-derived myeloid cells and further confirmed that some cell type-specific promoters remain methylated in the *AAVS1* safe harbor locus during differentiation. Thus, evaluation of different promoters might be necessary to avoid unexpected transgene silencing in the *AAVS1* locus.

Experimental procedures

Plasmids

The *AAVS1*-specific donor plasmid used for genetic correction was described elsewhere²⁵. Briefly, the donor plasmid consisted of two 750 bp homology arms including a splice acceptor site following a puromycin resistance cassette for selection of targeted clones and a bovine growth hormone polyadenylation signal for termination. The therapeutic codon-optimized cDNA for *NCF1* (synthesized by GeneArt/Thermo Fisher, Regensburg, Germany) was inserted into the donor plasmid via *Sall* and *PacI* restriction sites and was terminated by a herpes simplex virus thymidine kinase polyadenylation signal. The miR223 promoter was exchanged by the CatG/cFes and MRP8 promoter using *NotI* and *Sall* restriction sites (all restriction enzymes: New England Biolabs (NEB), Ipswich, MA).

The CRISPR-Cas9 plasmid carried a human U6 promoter to drive expression of the sgRNA. The 20 nucleotide long sgRNA target sequence for the *AAVS1* locus was cloned after phosphorylation and annealing of 100 pmol oligodeoxynucleotides 5'-AAVS1 (5'-CACCGTCACCAATCCTGTCCCTAG) and 100 pmol 3'-AAVS1 (5'-AAACCTAGGGACAGGATTGGTGAC) via two BsmBI restriction sites. Phosphorylation was performed at 37°C for 45 minutes using the T4 polynucleotide kinase (NEB) and annealing was achieved by incubation at 98°C for 150 seconds followed by a cool down to 22°C at a rate of -0.1°C/minute. Behind the sgRNA cassette, an SFFV promoter was cloned to drive expression of spCas9 and a dTomato fluorescence protein.

Cell culture

Human iPSC were cultivated on irradiated mouse embryonic fibroblasts C3H (MEF) as described before²⁶. The iPSC medium contained F12/DMEM medium (Gibco/Thermo Fisher, Waltham, MA) supplemented with 20% knockout serum replacement (Gibco/Thermo Fisher), 100 U/ml penicillin and 100 µg/ml streptomycin (PanBiotec, Aidenach, Germany), 2 mM L-glutamine (Biochrom, Berlin, Germany), 1% non-essential amino acids (Gibco/Thermo Fisher), 0.1 mM β-mercaptoethanol (Sigma-Aldrich, St. Louis, MO) and 20 ng/ml β-FGF (kindly provided by the Department of Technical Chemistry, Leibniz University Hannover). Once per week, colonies were picked onto new MEF in the presence of 10 µM ROCK inhibitor Y-27632 (Tocris, Bristol, UK). MEF were seeded one day in advance in low-glucose DMEM (PanBiotec) supplemented with 15% fetal bovine serum (FBS Standard, PanBiotec), 100 U/ml penicillin and 100 µg/ml streptomycin, 2 mM L-glutamine, 1% non-essential amino acids and 0.1 mM β-mercaptoethanol onto 0.1% bovine gelatin-coated plates (Sigma Aldrich).

Gene editing of iPSC

Two different p47^{phox}-deficient iPSC lines, p47-ΔGT (generated by CRISPR-Cas9 modification of healthy wild type (WT) iPSC derived from CD34⁺ cells) and p47-CGD (generated via reprogramming of peripheral blood from a CGD patient) were used in this study²⁷. For genetic correction, 5 x 10⁴ p47^{phox}-deficient iPSC were seeded in a 24-well plate on Geltrex (Thermo Fisher) in the presence of 10 µM ROCK inhibitor Y-27632. After 24 hours, 250 ng of the CRISPR-Cas9 plasmid and 250 ng of the donor plasmid were

This paper has been peer-reviewed and accepted for publication, but has yet to undergo copyediting and proof correction. The final published version may differ from this proof.

Human Gene Therapy

Differential transgene silencing of myeloid-specific promoters in the *AAVS1* safe harbor locus of iPSC-derived myeloid cells (DOI: 10.1089/hum.2019.194)

transfected using Lipofectamine Stem Reagent (Thermo Fisher). Briefly, 25 μ l F12/DMEM supplemented with 1 μ l Lipofectamine Stem Reagent were added to 25 μ l F12/DMEM mixed with 250 ng CRISPR-Cas9 plasmid and 250 ng donor plasmid. The mixture was incubated for 10 minutes at room temperature and added to the iPSC. After 24 hours, the iPSC were detached using trypsin (PanBiotech) and plated on puromycin-resistant DR4 MEF for selection. Single iPSC colonies were selected in iPSC medium supplemented with 0.2 μ g/ml puromycin (Invivogen, San Diego, CA) and analyzed for correct targeting.

Genetic analysis

Genomic DNA was isolated from all iPSC clones using the QIAamp DNA Blood Mini Kit (Qiagen, Hilden, Germany). All PCRs were performed using the Phusion Green Hot Start II High-Fidelity PCR Master Mix (Thermo Fisher). The 5'-junction of the inserted donor construct was amplified with primers 5F (5'-GACCTGCATTCTCTCCCTGG) and 5R (5'-GGGCTTGACTCGGTCATCTCG) (930 bp amplicon). The 3'-junction was amplified using primers 3F (5'-CCAAGTTCGGGTGAAGGCC) and 3R (5'-AAGCCTGAGCGCCTCTCCTG) (846 bp amplicon). Random insertion of the donor plasmid was addressed by amplifying the 5'- and 3'-termini of the plasmid with primers D5F (5'-GGGTGTCGGGGCTGGCTTAAC) and 5R (961 bp amplicon) and with primers D3F (5'-GTGAGAATGGTGCCTCCTAGG) and D3R (5'-TATAGTCTGTCGGGTTTCGCC) (684 bp amplicon), respectively. Monoallelic or biallelic targeting was assessed by amplification of wild type sequence around the Cas9 cleavage site using primers WF (5'-GACAGCATGTTTGCTGCCTCC) and WR (5'-GGATCCTCTCTGGCTCCATCG) (320 bp amplicon). All PCR products were analyzed by electrophoresis on 1% agarose gels (Invitrogen/Thermo Fisher).

Myeloid differentiation of iPSC

All iPSC clones were differentiated into the myeloid/granulocytic lineage using an embryoid body (EB)-based protocol as previously described²⁸. Briefly, iPSC colonies were grown to high density and detached using dispase (Roche, Basel, Switzerland). The colonies were transferred into EB medium (KO/DMEM medium (Gibco/Thermo Fisher) supplemented with 20% knockout serum replacement, 100 U/ml penicillin and 100 μ g/ml streptomycin, 2 mM L-glutamine, 1% non-essential amino acids, 0.1 mM β -mercaptoethanol and 10 μ M ROCK inhibitor Y-27632. After 5 days on an orbital shaker at

80 rpm, EB were picked into APEL2 medium (StemCell Technologies, Vancouver, Canada) supplemented with 100 U/ml penicillin and 100 µg/ml streptomycin, 50 ng/ml human granulocyte colony-stimulating factor (G-CSF, Peprotech, Rocky Hill, NJ) and 25 ng/ml human interleukin-3 (IL-3, Peprotech). Differentiated cells were harvested once per week and cultured in RPMI 1640 medium (PanBiotech) supplemented with 10% FBS, 100 U/ml penicillin and 100 µg/ml streptomycin, 2 mM L-glutamine and 100 ng/ml G-CSF.

Myeloid cell morphology was analyzed by Pappenheim staining. About 5×10^4 differentiated cells were spun onto microscope glass slides using a Cytospin 4 (Thermo Scientific). After May-Grünwald and Giemsa staining according to manufacturer's instructions (Pappenheim staining, Sigma-Aldrich), cells were analyzed with an Olympus BX51 microscope (software Cell[^]F version 3.4, Olympus, Tokyo, Japan).

Differentiated cells were analyzed for surface marker expression by flow cytometry (CytoFlex S, Beckman Coulter, Brea, CA) using the following antibodies: CD45-FITC (Clone: 5B1, Miltenyi, Bergisch-Gladbach, Germany), CD11b-PE (Clone: M1/70.15.11.5, Miltenyi), CD66b-APC (Clone: G10F5, Biolegend, SanDiego, CA) and the viability dye DAPI (Sigma Aldrich). Prior to antibody staining, cells were blocked with human FcR blocking reagent (Miltenyi).

Intracellular p47^{phox} staining

Myeloid cells were fixed and permeabilized using the FoxP3 intracellular staining kit (Biolegend). Briefly, fixation was performed for 20 minutes in Fix/Perm solution. After washing once with PBS and once with Perm buffer, the cells were incubated in Perm buffer for 15 minutes. Primary p47^{phox} antibody (BD, Franklin Lakes, NJ) staining was done for 30 minutes followed by 30 minutes incubation with a goat-anti-mouse DyLight488 secondary antibody (Thermo Fisher). Data was acquired using a CytoFlex S flow cytometer.

Bisulfite Sequencing

Genomic DNA from iPSC and myeloid cells was isolated using the QIAamp DNA Blood Mini Kit. Bisulfite conversion was performed using the EpiTect Bisulfite Kit (Qiagen) according to manufacturer's instructions. For the bisulfite conversion, 20 µl genomic DNA was mixed with 85 µl bisulfite mix and 35 µl DNA Protect Buffer and incubated for 5 minutes at 95°C, 25 minutes at 60°C, followed by another 5 minutes at 95°C, 85 minutes at 60°C, 5 minutes

at 95°C and finally 175 minutes at 60°C. After cleanup of the bisulfite converted DNA using spin columns, the promoter sequences for miR223, CatG/cFes and MRP8 were amplified by semi-nested PCR using a Taq polymerase (Qiagen). The respective primers are listed in Table 1. All PCR products were isolated from a 1% agarose gel and cloned into pCR2.1 plasmid via TA cloning. Five colonies were picked from each plate for plasmid isolation. The plasmid was Sanger sequenced using the M13 primer (5'-TGAAAACGACGGCCAGT).

Dihydrorhodamine (DHR) assay

The DHR assay was performed as previously described²⁵, with minor modifications. Briefly, 10⁵ cells were stimulated with 40 nM phorbol 12-myristate 13-acetate (PMA; Sigma Aldrich) in the presence of 1000 U catalase (Sigma Aldrich) in 500 µl Hank's Buffered Salt Solution (HBSS) containing Mg/Ca (Gibco / Thermo Fisher). After stimulation for 5 minutes, 250 ng DHR (Sigma Aldrich) was added to the cells for 15 minutes. The reaction was stopped by placing the cells on ice. Data was recorded by flow cytometry (CytoFlex S).

Statistical analysis

Statistical significance was determined using one-way ANOVA with GraphPad Prism 7. All bar graphs represent the mean ± SD. ***P≤0.001, ****P≤0.0001.

Results

Targeting the AAVS1 safe harbor locus for correction of p47-CGD

The overall aim of this study was to correct p47^{phox}-deficiency by insertion of a therapeutic codon-optimized *NCF1* cDNA into the *AAVS1* safe harbor locus using CRISPR-Cas9. To maintain myeloid-specific expression of p47^{phox}, we tested three different myeloid-specific promoters: miR223, CatG/cFes and MRP8 (Figure 1A). Prior to targeting the *AAVS1* locus in iPSC, we used a fluorescence reporter assay in HT1080 cells to determine the on-target activity of the applied sgRNA. The reporter construct consisted of a super-folder green fluorescent protein (sfGFP), which contained the sgRNA target sequence behind the ATG start codon of sfGFP (Figure S1A). We used lentiviral vectors for the delivery of the CRISPR-Cas9 system to mediate efficient gene transfer and to track genetically modified cells via the dTomato fluorescent protein on the CRISPR-Cas9 construct (Figure S1A). After delivery of the CRISPR-Cas9 components and cleavage of the target sequence, the induced DSB

10

were repaired by non-homologous end-joining. In about 66% of cleaved alleles, the repair would result in a frameshift and a subsequent loss of sfGFP fluorescence, which can be detected via flow cytometry. We measured an on-target activity of 43-47% on average for the AAVS1-specific sgRNA at different multiplicities of infection (Figure S1B-S1D). After validation of the sgRNA, two different $p47^{\text{phox}}$ -deficient iPSC lines ($p47\text{-}\Delta\text{GT}$ generated by CRISPR-Cas9 and $p47\text{-CGD}$ generated via reprogramming²⁷) were corrected by applying the different donor constructs and the CRISPR-Cas9 plasmid via lipofection. We identified a biallelic corrected clone for each promoter construct and each iPSC clone ($p47\text{-}\Delta\text{GT}$: miR223 #4, CatG/cFes #5, MRP8 #16, $p47\text{-CGD}$: miR223 #4, CatG/cFes #12, MRP8 #12) via PCR screening for the 5'- and 3'-junction site and the wild type sequence around the Cas9 cleavage site (Figure 1B,C). Random insertion of the donor plasmid in selected clones was excluded by two additional PCR amplifications for the 5'- and 3'-side of the donor plasmid. The screening results of all analyzed iPSC clones were summarized in Figure 1D. In most cases, we achieved more monoallelic corrected clones than biallelic corrected clones most likely due to the low frequency of HDR. We observed between 40% and 80% random insertion of the donor plasmid, which might be due to an excessive amount of donor plasmid in the transfection reaction. All gene-edited iPSC clones maintained their typical iPSC morphology (Figure S2A). Moreover, surface staining revealed expression of the pluripotency markers SSEA-4 and TRA-1-60 in all iPSC clones, which confirmed that they remained pluripotent after gene editing (Figure S2B). Finally, quantitative PCR demonstrated similar expression of the pluripotency genes *OCT4*, *NANOG* and *DNMT3B* compared to embryonic stem cells (Figure S2C). In summary, we genetically corrected two different $p47^{\text{phox}}$ -deficient iPSC lines by insertion of a codon-optimized *NCF1* minigene into the *AAVS1* safe harbor locus.

Differentiated myeloid cells had restored $p47^{\text{phox}}$ expression and functional NADPH oxidase activity

To analyze $p47^{\text{phox}}$ expression, all iPSC clones were differentiated into myeloid cells using an EB-based differentiation protocol²⁸. To drive the differentiation into the granulocytic lineage, we added G-CSF and IL-3 to the hematopoietic differentiation medium. Staining of differentiated cells with May-Grünwald and Giemsa revealed segmented neutrophils as

well as myeloid progenitors (Figure 2A). Macrophages were also observed in many differentiations, but there was great variation regarding the amount of macrophages produced among different experiments. Further characterization of the differentiated myeloid cells by staining for the surface markers CD45, CD11b and CD66b, revealed 91-99% CD45-positive cells (Figure 2B). These cells were 80-94% CD11b-positive and 26-46% double-positive for CD11b and CD66b (Figure 2C).

Restored p47^{phox}-expression was assessed via intracellular staining in the parental iPSC and the differentiated CD45⁺ myeloid cells. As expected in iPSC, the wild type and corrected clones lacked p47^{phox} expression as did the p47^{phox}-deficient iPSC lines (Figure 3A). In differentiated myeloid cells, p47^{phox} expression from the miR223 promoter was similar to wild type cells ($66.3 \pm 7.4\%$ p47^{phox}-positive cells) and in the range of $57.3 \pm 21.6\%$ p47^{phox}-positive cells (Figure 3B,C). The p47^{phox} expression from the CatG/cFes promoter ranged from $19.5 \pm 13.6\%$ p47^{phox}-positive cells, while the MRP8 promoter resulted in only $6.9 \pm 6.5\%$ p47^{phox}-positive myeloid cells. These findings indicated strong differences in the activities of various promoters and that expression from the myeloid-specific promoters was restricted to differentiated myeloid cells with no leakiness observed in iPSC. We also compared the p47^{phox} expression in some clones with a monoallelic correction to the clones with the biallelic correction and observed similar expression levels (Figure 3C).

Functional NADPH oxidase activity was assessed in a dihydrorhodamine (DHR) assay, which detected ROS production by the conversion of DHR into green-fluorescent rhodamine (Rho) 123. As expected, all iPSC clones failed to produce ROS in this assay due to the fact that the components of the NADPH oxidase are not expressed in iPSC (Figure 4A). Upon differentiation, cells corrected with the miR223 promoter yielded $73.9 \pm 18.3\%$ Rho123-positive cells, which was slightly below wild type levels ($93.5 \pm 2.8\%$ Rho123-positive cells) (Figure 4B,C). The CatG/cFes promoter yielded $18.6 \pm 13.0\%$ Rho123-positive cells, which was again inferior to the miR223 promoter but higher compared to the MRP8 promoter ($6.3 \pm 4.3\%$ Rho123-positive cells). Taken together, differentiated myeloid cells derived from corrected iPSC revealed restored NADPH oxidase activity, which reflected the p47^{phox} expression levels (Figure 3C). In contrast to the MRP8 promoter, cells corrected with the miR223 and CatG/cFes promoter expressed therapeutically relevant levels of p47^{phox} and

12

restored NADPH oxidase activity. The miR223 promoter achieved the highest levels of p47^{phox} expression and was comparable to wild type cells.

Myeloid-specific promoters were differentially silenced in the AAVS1 safe harbor locus

To analyze whether promoter silencing in the *AAVS1* locus had an effect on the transgene expression, we performed bisulfite sequencing of the myeloid-specific promoters in iPSC and in the differentiated myeloid cells to assess the DNA methylation status, which is a good predictor of gene expression²⁹. Based solely on promoter sequence, all three myeloid-specific promoters contain different amounts of CpGs that could be potentially methylated. While the miR223 promoter contained only four CpGs, the CatG/cFes promoter had 52 CpGs and the MRP8 promoter had 13 CpGs. Due to a high CpG density and a CpG island in the 3'-part of the CatG/cFes promoter, we only analyzed the first 12 CpGs of the CatG/cFes promoter, which covered the first half of the promoter. We observed extensive (85-98%) CpG methylation of all promoters in iPSC (Figure 5A-C). Upon myeloid differentiation, the promoter methylation status decreased to 20-25% for the miR223 promoter, 8-40% for the CatG/cFes promoter and 64-80% for the MRP8 promoter. In conclusion, we observed that the analyzed myeloid-specific promoters were mainly methylated in the *AAVS1* safe harbor locus of iPSC and demethylated to different extents upon myeloid differentiation.

Discussion

The *AAVS1* locus has been described as a genomic safe harbor with open and active chromatin that allows higher expression of an inserted transgene compared to the *CCR5* gene⁸. However, we and others showed that certain cell type-specific promoters, when integrated into the *AAVS1* locus, become methylated and mediate low transgene expression in differentiated cells²¹. In our study, we tested three different myeloid-specific promoters (miR223, CatG/cFes and MRP8) to drive expression of a therapeutic *NCF1* cassette in the *AAVS1* locus. In the context of iPSC-derived myeloid cells, we demonstrated that the miR223 and CatG/cFes promoter achieved therapeutically relevant transgene expression levels and NADPH oxidase activity. In a study by Merling *et al.*, the authors targeted the *AAVS1* locus with a constitutively expressing CAG promoter to drive expression of p47^{phox} in patient-derived iPSC³⁰. Upon differentiation, only 26% Rho123-

positive cells were generated from p47^{phox}-corrected granulocytes in the earlier study. The authors claimed that this low rate was caused by variable differentiation rates and probably a low yield of myeloid cells in that specific assay. However, for other CGD lines, the authors measured up to 90% Rho123-positive cells using the CAG promoter, which is comparable to our data with the miR223 promoter. Brendel *et al.* compared the expression strength of the miR223 promoter to other myeloid-specific promoters, including the cFes and MRP8 promoter²². In their comparison, they observed superior performance of the miR223 promoter compared to the other promoters in regard to p47^{phox} induction and Rho123-positive cells in differentiated murine granulocytes. Although the degree of epigenetic modifications might differ between murine hematopoietic stem and progenitor cells and iPSC, the expression strength of the miR223 promoter in comparison to the MRP8 promoter in murine granulocytes was quite similar to our data in iPSC-derived myeloid cells.

To maintain pluripotency, pluripotent stem cells possess a unique DNA methylation profile^{29,31}. In general, DNA methylation plays an important role in establishing and maintaining tissue-specific gene expression and correlates inversely with gene expression³². We observed that all three myeloid-specific promoters were highly methylated in the iPSC state, in which the promoters are inactive. The differentiation of pluripotent stem cells is associated with extensive epigenetic reprogramming that involves changes in DNA methylation, binding of transcription factors and modification of DNA-binding proteins, which changes the chromatin structure and makes it accessible for the transcription machinery³³. Upon myeloid differentiation, we measured a different degree of demethylation for the promoters tested in this study, which in turn partly correlated with the observed transgene expression. We observed quite heterogeneous results for the CatG/cFes promoter with regard to p47^{phox} expression levels and the methylation status in the two different iPSC lines. Despite 40% CpG methylation in the 5'-part of the promoter in p47-CGD CatG/cFes clone #12, we achieved up to 40% p47^{phox} expression and NADPH oxidase activity. In contrast, p47-ΔGT CatG/cFes clone #5 that had 8% methylated CpGs yielded only 15% p47^{phox} expression and NADPH oxidase activity. Moreover, the demethylation of the myeloid-specific promoters could be completely different when targeting primary HSC. So far, methylation of the CatG/cFes promoter has not been

observed in neutrophils of CGD patients that were treated with gene therapy (unpublished data). Although it has been described that the MRP8 promoter relies on methylation of certain CpGs to bind specific transcription factors and to drive expression, it performed very poorly in our assays despite high DNA methylation³⁴. Also in the context of lentiviral vectors, the MRP8 promoter shows a high abundance of repressive histone marks and low transgene expression in iPSC-derived myeloid cells³⁴. The inclusion of insulators or ubiquitous chromatin opening elements (UCOE), such as the 1.8 kb element or a shortened CBX3 version, could help to overcome transgene silencing^{21,34-36}. Insulators are DNA sequences that block the spread of heterochromatin and thus protect against silencing and DNA methylation³⁷. Ordovàs *et al.* observed that the OCT4 promoter, which was inactive in the *AAVS1* locus without insulators, had 100% transgene expression when flanked by insulator sequences²¹. However, others demonstrated that mosaicism can occur in a safe harbor locus even with insulators, e.g. the murine *Rosa26* and *Col1A1* genes^{38,39}. Insertion of a CBX3 element upstream of the internal promoter can also protect against epigenetic transgene silencing and stabilize expression of transgenes that are integrated into the genome. Müller-Kuller *et al.* showed that the addition of CBX3 next to the MRP8 promoter increased transgene expression by two-fold in iPSC-derived myeloid cells and the expression intensity by five-fold in a myelomonocytic cell line³⁴.

We conclude that the targeted integration of a therapeutic transgene into a genomic safe harbor locus can reduce the risk of insertional mutagenesis compared to semi-randomly integrating vectors. However, the criteria of predictable transgene function do not apply without restrictions as sequence-dependent transgene silencing can occur in the *AAVS1* safe harbor locus in human pluripotent stem cells²¹. Here, we tested three different myeloid-specific promoters that were integrated into the *AAVS1* locus and observed that the miR223 promoter performed highly reliably, with corrected cells producing similar NADPH oxidase activity compared to wild type cells. The CatG/cFes promoter also allowed stable and therapeutically relevant p47^{phox} expression levels in iPSC-derived myeloid cells, whereas the MRP8 promoter was prone to silencing. Thus, the correct promoter choice is essential to achieve sufficient gene expression, e.g. in a therapeutic setting. Moreover, the inclusion of insulators and UCOE could help to overcome transgene silencing for promoters

that are prone to epigenetic silencing via DNA methylation or addition of repressive histone marks.

Acknowledgement

This work was supported by grants from the German Research Foundation (SFB738 (C9) and REBIRTH Cluster of Excellence (EXC 62)), the Federal Ministry of Education and Research (Pidnet (FK2016M1517F)), the German Academic Scholarship Foundation and furthermore this project has received funding from the European Union's Horizon 2020 research and innovation programme under grant agreement No 666908. A.J.T. and G.S. were supported by the Wellcome Trust (104807/Z/14/Z) and the NIHR Biomedical Research Centre at Great Ormond Street Hospital for Children NHS Foundation Trust and University College London. We thank Michael Morgan for proof-reading the manuscript (Hannover Medical School, Germany), Toni Cathomen for providing the AAVS1-specific donor plasmid (University Freiburg, Germany) and Tobias Cantz for providing the mouse embryonic feeder cells (Hannover Medical School, Germany).

Author Disclosure

The authors declare no conflict of interest.

References

1. Pickar-Oliver A, Gersbach CA. The next generation of CRISPR-Cas technologies and applications. *Nat Rev Mol Cell Biol* 2019;8:490-507.
2. Ott MG, Schmidt M, Schwarzwaelder K, et al. Correction of X-linked chronic granulomatous disease by gene therapy, augmented by insertional activation of MDS1-EVI1, PRDM16 or SETBP1. *Nat Med* 2006;12:401-409.
3. Stein S, Ott MG, Schultze-Strasser S, et al. Genomic instability and myelodysplasia with monosomy 7 consequent to EVI1 activation after gene therapy for chronic granulomatous disease. *Nat Med* 2010;16:198-204.
4. Hacein-Bey-Abina S, von Kalle C, Schmidt M, et al. A serious adverse event after successful gene therapy for X-linked severe combined immunodeficiency. *N Engl J Med* 2003;348:255-256.
5. Wu C, Dunbar C. Stem cell gene therapy: the risks of insertional mutagenesis and approaches to minimize genotoxicity. *Front Med* 2011;5:356-371.
6. Howe SJ, Mansour MR, Schwarzwaelder K, et al. Insertional mutagenesis combined with acquired somatic mutations causes leukemogenesis following gene therapy of SCID-X1 patients. *J Clin Invest* 2008;118:3143-3150.
7. Papapetrou EP, Schambach A. Gene Insertion Into Genomic Safe Harbors for Human Gene Therapy. *Mol Ther* 2016;24:678-684.
8. Lombardo A, Cesana D, Genovese P, et al. Site-specific integration and tailoring of cassette design for sustainable gene transfer. *Nat Methods* 2011;8:861-869.
9. Sadelain M, Papapetrou EP, Bushman FD. Safe harbours for the integration of new DNA in the human genome. *Nat Rev Cancer* 2012;12:51-58.

10. Roos D. The genetic basis of chronic granulomatous disease. *Immunol Rev* 1994;138:121-157.
11. Roos D. Chronic granulomatous disease. *Br Med Bull* 2016;118:50-63.
12. Segal BH, Leto TL, Gallin JI, et al. Genetic, biochemical, and clinical features of chronic granulomatous disease. *Medicine* 2000;79:170-200.
13. van den Berg JM, van Koppen E, Ahlin A, et al. Chronic granulomatous disease: the European experience. *PLoS ONE* 2009;4:e5234.
14. Heyworth PG, Cross AR, Curnutte JT. Chronic granulomatous disease. *Curr Opin Immunol* 2003;15:578-584.
15. Brunson T, Wang Q, Chambers I, et al. A copy number variation in human NCF1 and its pseudogenes. *BMC Genet* 2010;11:13.
16. Hayrapetyan A, Dencher PC, Leeuwen Kv, et al. Different unequal cross-over events between NCF1 and its pseudogenes in autosomal p47(phox)-deficient chronic granulomatous disease. *Biochim Biophys Acta* 2013;1832:1662-1672.
17. Chanock SJ, Roesler J, Zhan S, et al. Genomic Structure of the Human p47-phox (NCF1) Gene. *Blood Cells Mol Dis* 2000;26:37-46.
18. Roesler J, Curnutte JT, Rae J, et al. Recombination events between the p47-phox gene and its highly homologous pseudogenes are the main cause of autosomal recessive chronic granulomatous disease. *Blood* 2000;95:2150-2156.
19. Roos D, Kuhns DB, Maddalena A, et al. Hematologically important mutations: the autosomal recessive forms of chronic granulomatous disease (second update). *Blood Cells Mol Dis* 2010;44:291-299.

20. Merling RK, Kuhns DB, Sweeney CL, et al. Gene-edited pseudogene resurrection corrects p47phox-deficient chronic granulomatous disease. *Blood Adv* 2017;1:270-278.
21. Ordovás L, Boon R, Pistoni M, et al. Efficient Recombinase -Mediated Cassette Exchange in hPSCs to Study the Hepatocyte Lineage Reveals AAVS1 Locus -Mediated Transgene Inhibition. *Stem Cell Reports* 2015;5:918-931.
22. Brendel C, Hänseler W, Wohlgensinger V, et al. Human miR223 promoter as a novel myelo-specific promoter for chronic granulomatous disease gene therapy. *Hum Gene Ther Methods* 2013;24:151-159.
23. Santilli G, Almarza E, Brendel C, et al. Biochemical Correction of X-CGD by a Novel Chimeric Promoter Regulating High Levels of Transgene Expression in Myeloid Cells. *Mol Ther* 2011;19:122-132.
24. Brendel C, Müller-Kuller U, Schultze-Strasser S, et al. Physiological regulation of transgene expression by a lentiviral vector containing the A2UCOE linked to a myeloid promoter. *Gene Ther* 2012;19:1018-1029.
25. Dreyer A, Hoffmann D, Lachmann N, et al. TALEN-mediated functional correction of X-linked chronic granulomatous disease in patient-derived induced pluripotent stem cells. *Biomaterials* 2015;69:191-200.
26. Philipp F, Selich A, Rothe M, et al. Human Teratoma-Derived Hematopoiesis Is a Highly Polyclonal Process Supported by Human Umbilical Vein Endothelial Cells. *Stem Cell Reports* 2018;11:1051-1060.
27. Klatt D, Cheng E, Philipp F, et al. Targeted Repair of p47-CGD in iPSCs by CRISPR/Cas9: Functional Correction without Cleavage in the Highly Homologous Pseudogenes. *Stem Cell Reports* 2019;13:590–8.

28. Lachmann N, Ackermann M, Frenzel E, et al. Large -Scale Hematopoietic Differentiation of Human Induced Pluripotent Stem Cells Provides Granulocytes or Macrophages for Cell Replacement Therapies. *Stem Cell Reports* 2015;4:282-296.
29. Altun G, Loring JF, Laurent LC. DNA methylation in embryonic stem cells. *J Cell Biochem* 2010;109:1-6.
30. Merling RK, Sweeney CL, Chu J, et al. An AAVS1-targeted minigene platform for correction of iPSCs from all five types of chronic granulomatous disease. *Mol Ther* 2015;23:147-57.
31. Bibikova M, Chudin E, Wu B, et al. Human embryonic stem cells have a unique epigenetic signature. *Genome Res* 2006;16:1075-1083.
32. Han H, Cortez CC, Yang X, et al. DNA methylation directly silences genes with non-CpG island promoters and establishes a nucleosome occupied promoter. *Hum Mol Genet* 2011;20:4299-4310.
33. Zhao MT, Shao NY, Hu S, et al. Cell Type-Specific Chromatin Signatures Underline Regulatory DNA Elements in Human Induced Pluripotent Stem Cells and Somatic Cells. *Circ Res* 2017;121:1237-1250.
34. Müller-Kuller U, Ackermann M, Kolodziej S, et al. A minimal ubiquitous chromatin opening element (UCOE) effectively prevents silencing of juxtaposed heterologous promoters by epigenetic remodeling in multipotent and pluripotent stem cells. *Nucleic Acids Res* 2015;43:1577-1592.
35. Ackermann M, Lachmann N, Hartung S, et al. Promoter and lineage independent anti-silencing activity of the A2 ubiquitous chromatin opening element for optimized human pluripotent stem cell-based gene therapy. *Biomaterials* 2014;35:1531-1542.
36. Kunkiel J, Gödecke N, Ackermann M, et al. The CpG-sites of the CBX3 ubiquitous chromatin opening element are critical structural determinants for the anti-silencing function. *Sci Rep* 2017;7:7919-13.

37. Dickson J, Gowher H, Strogantsev R, et al. VEZF1 elements mediate protection from DNA methylation. *PLoS Genet* 2010;6:e1000804.
38. Haenebalcke L, Goossens S, Naessens M, et al. Efficient ROSA26-based conditional and/or inducible transgenesis using RMCE-compatible F1 hybrid mouse embryonic stem cells. *Stem Cell Rev* 2013;9:774-785.
39. Beard C, Hochedlinger K, Plath K, et al. Efficient method to generate single-copy transgenic mice by site-specific integration in embryonic stem cells. *Genesis* 2006;44:23-28.

Table 1: Primer sequences used for bisulfite sequencing

Primer	Sequence (5'-3')
miR223_1_fw	TGATTTGTATAGTTTTATAGGGTTTTATGTTTAGAAG
miR223_1_rev_1	TAAAAAAACCCRTAATCAAATTAAAAAACAAAACCTC
miR223_1_rev_2	CCCCATAAACTCCAAATCACATATTCTTTCACTC
miR223_2_fw	GAGTCAAAGAATATGTGATTTGGAGTTTATGGGG
miR223_2_rev_1	CAAACTACAAAAAATAAAAAACACCTAAC
miR223_2_rev_2	AAACACCTAACTACCCTAACTCTACCTATAAATC
miR223_3_fw	GGTTTGTATTATTGTTGTAGTAGATTTTTTTTAT
miR223_3_rev_1	AAACCAACAAAACAATATATCTAATAAAAAATA
miR223_3_rev_2	TACCTTAATCATAAAAAAACTCTAATTCCCC
CatG/cFes_1_fw_1	TTTTTGTGTTTGGAGTATTTTGAATTTG
CatG/cFes_1_fw_2	TTTTTTTTTGTGTTGGGTTTTTATTTTTG
CatG/cFes_1_rev	CACAATCCCATTCTCTACTACCATAAAAAATT
CatG/cFes_2_fw_1	AATTTTTTATGGTAGTAGGAGAATGGGATTGTG
CatG/cFes_2_fw_2	TTAGGAGGAGGGAGTATAGTAGTAATTGATTGGG
CatG/cFes_2_rev	AAACCCCAAACAATACTAAACCCAAAAAAACCC
CatG/cFes_3_fw_1	TTGGGATTAGGGTTTTTTTTTTTTTTTTTTT
CatG/cFes_3_fw_2	GGGTTTTTTGGGTTTAGTATTTGTTTGGGGTTT
CatG/cFes_3_rev	AAACCAACAAAACAATATATCTAATAAAAAATA
MRP8_1_fw	TAAGGGGGAGGATTGGGAAGATAATAGTAGGTATG
MRP8_1_rev_1	CCAAAATATAAAAAAATCCCTACAACCTCAACAACA
MRP8_1_rev_2	CCAATCAAAAATTAAAAAAATACTCAAATAAACACT
MRP8_2_fw_1	GTGGGGAGAGGATTTGTTTTTTTTGAAATTTGGGG
MRP8_2_fw_2	TGGGGAATTGGTTATTTTTTTTTTTTTTTTAGGTATG
MRP8_2_rev	CCTATTCTATAAACTAAAAATAAACCATACCCTAA
MRP8_3_fw_1	TTAGGGTATGGTTATTTTTTAGTTTTATAGAATAGG
MRP8_3_fw_2	TAGGGTAGGAATGGATATAGTTTTTGG
MRP8_3_rev	TCATTTTAAATACATACACTCAATAAAAAACATTCCTCC
MRP8_4_fw_1	TGGAGGAATGTTTTATTGAGTGTATG

MRP8_4_fw_2	TGATGTATTTAATTTAATTTAGTTTTAGGGATGTATG
MRP8_4_rev	TCAAAAACAACCTCTCCCTACCAAATTAC
MRP8_5_fw_1	TTGGTTGAGAAATTAGAGATTGTAGTAATTTTGG
MRP8_5_fw_2	GTAATTTTGGTAGGGAGAAGTTGTTTTTGA
MRP8_5_rev	CCACCTTCTCGCTCAAATCCTACCACTTCAC

Figure 1. Targeting the *AAVS1* locus for genetic correction of p47- Δ GT and p47-CGD iPSC.

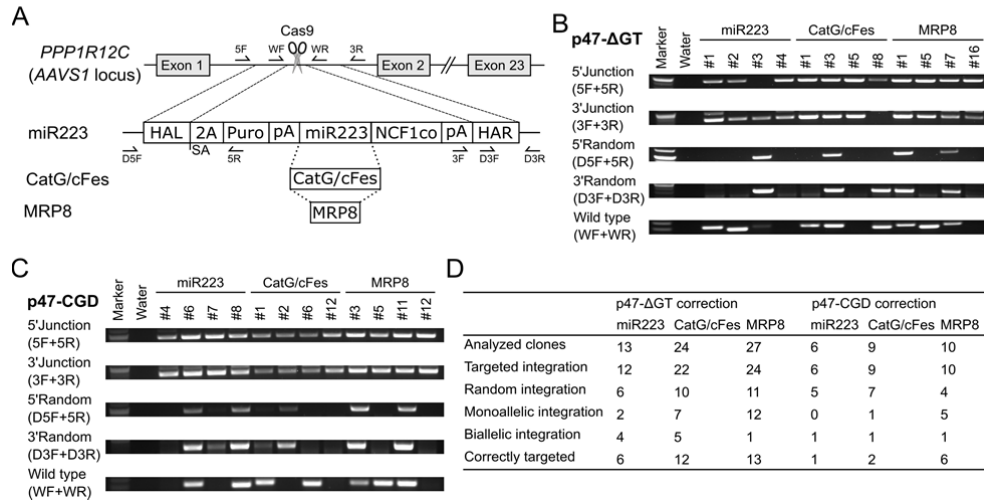


Figure 1. Targeting the *AAVS1* locus for genetic correction of p47- Δ GT and p47-CGD iPSC.

(A) Schematic of the *AAVS1* safe harbor locus and the gene correction strategy for p47^{phox} deficiency. The Cas9 is guided to intron 1 of *PPP1R12C* (*AAVS1* locus) and introduces a DNA double strand break, which induces homology-directed repair via the donor template. F, forward primer; R, reverse primer; HAL, homology arm left; SA, splice acceptor site; 2A, peptide cleavage site; Puro, puromycin resistance gene; pA, polyadenylation signal; NCF1co, codon-optimized cDNA encoding *NCF1* gene; HAR, homology arm right. The arrows indicate primer binding sites used for PCR-based screening of corrected iPSC clones. **(B)** PCR-based screening to identify corrected p47- Δ GT clones. The primers were used as indicated in (A). **(C)** PCR-based screening to identify corrected p47-CGD clones. **(D)** Quantitative analysis of gene correction and random integration summarized from all analyzed p47- Δ GT and p47-CGD iPSC clones.

Figure 2. Myeloid differentiation of corrected iPSC clones.

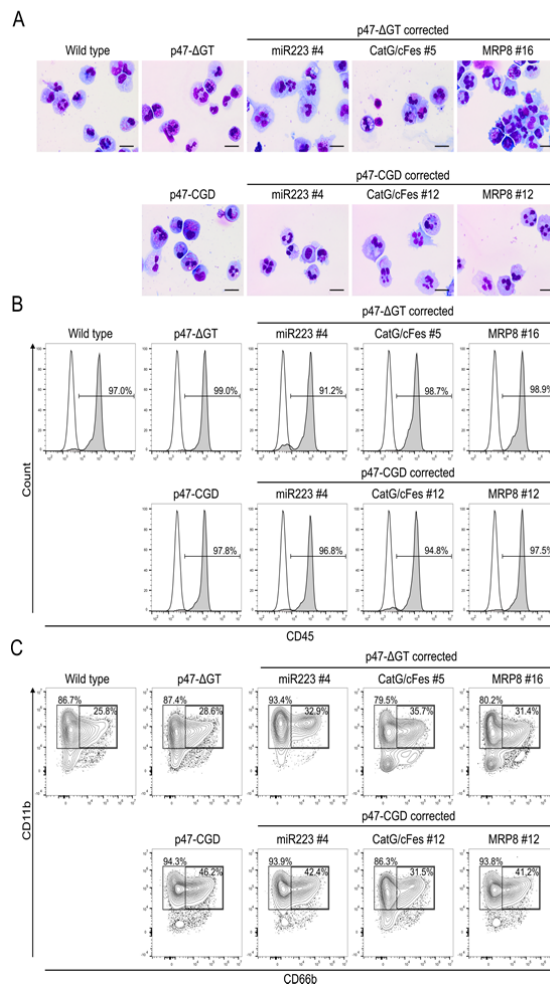
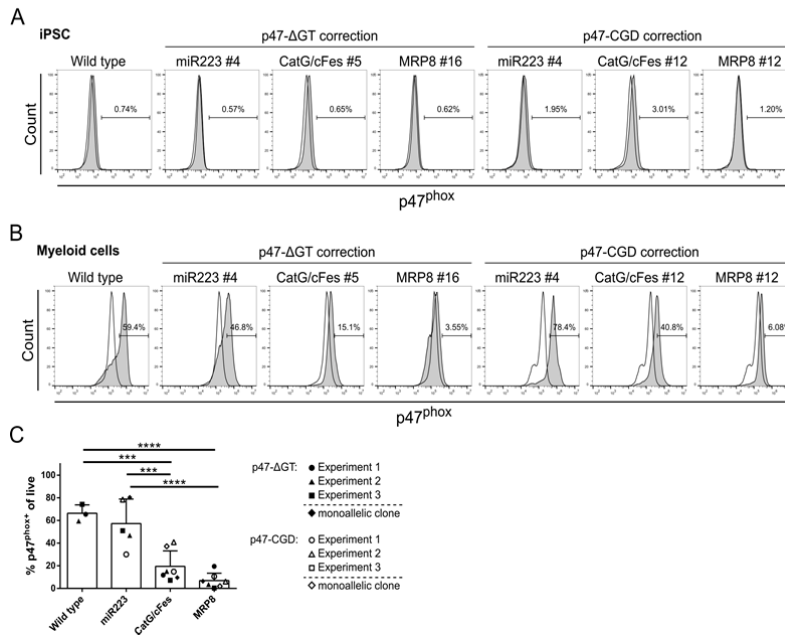


Figure 2. Myeloid differentiation of corrected iPSC clones.

(A) All iPSC clones were differentiated into myeloid cells. Cytopins from corrected iPSC-derived myeloid cells were stained with Papanheim staining solutions to assess the cell morphology of differentiated cells (scale bar = 20 μ m). **(B)** Differentiated iPSC-derived myeloid cells were stained for the hematopoietic marker CD45. The expression was analyzed in viable cells by flow cytometry. Black line = isotype control, gray = stained cells. **(C)** Upon surface marker staining, the expression of the myeloid marker CD11b and the granulocytic marker CD66b was measured in CD45⁺ iPSC-derived myeloid cells by flow cytometry. Representative FACS plots of three independent experiments/differentiations are shown.

Figure 3. Differentiated myeloid cells had restored p47^{phox} expression.Figure 3. Differentiated myeloid cells had restored p47^{phox} expression.

(A) All iPSC clones were stained intracellularly for p47^{phox}. The expression of p47^{phox} was analyzed in viable iPSC by flow cytometry. Data represent one independent experiment. As negative control, the parental p47^{phox}-deficient iPSC were used, which received the whole antibody staining. The gating is based on the respective parental p47^{phox}-deficient p47-ΔGT (also for wild type) or p47-CGD clone. Black line = stained negative control, gray = stained samples. **(B)** After myeloid differentiation all clones were stained for p47^{phox}. Upon intracellular antibody staining, p47^{phox} expression was measured in CD45⁺ iPSC-derived myeloid cells via flow cytometry. Representative histograms of three independent experiments/differentiations are shown. As negative control, the parental p47^{phox}-deficient iPSC-derived CD45⁺ myeloid cells were used, which received complete antibody staining. The gating is based on the respective parental p47^{phox}-deficient p47-ΔGT (also for wild type) or p47-CGD clone. Black line = stained negative control, gray = stained samples. **(C)** The bar graph summarizes p47^{phox} expression in corrected p47-ΔGT (black symbols) and p47-CGD clones (white symbols) from three independent differentiations. Diamonds represent monoallelic corrected clones (n = 3-7, mean ± SD, statistics: one-way ANOVA, *** p<0.001, **** p<0.0001).

Figure 4. Corrected myeloid cells had functional NADPH oxidase activity.

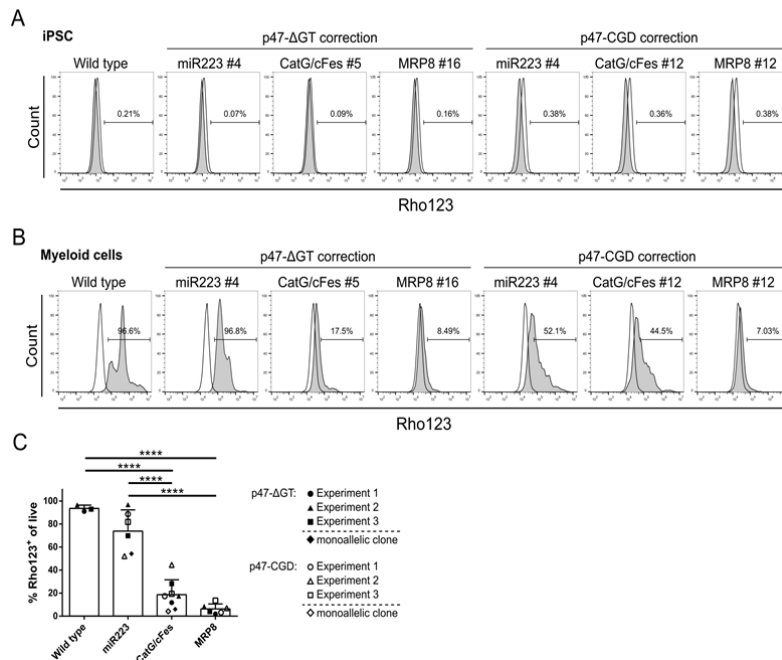


Figure 4. Corrected myeloid cells had functional NADPH oxidase activity.

(A) The dihydrorhodamine (DHR) assay was performed on undifferentiated iPSC. Upon phorbol 12-myristate 13-acetate (PMA) stimulation, DHR is converted into green fluorescent Rho123 in the presence of reactive oxygen species. The frequency of Rho123⁺ cells was analyzed in viable iPSC by flow cytometry. Unstimulated cells were used as a negative control. Black line = unstimulated cells, gray = stimulated cells. Histograms represent one independent experiment. **(B)** The DHR assay was performed on iPSC-derived myeloid cells. The frequency of Rho123⁺ cells was analyzed in CD45⁺ myeloid cells by flow cytometry. As negative control, stimulated p47^{phox}-deficient myeloid cells (p47-ΔGT or p47-CGD) were used. The gating is based on the respective parental p47^{phox}-deficient p47-ΔGT (also for wild type) or p47-CGD clone. Black line = stimulated negative control, gray = stimulated wild type and corrected cells. Representative histograms of three independent experiments/differentiations are depicted. **(C)** The bar graph represents the results of all DHR assays performed on corrected p47-ΔGT (black symbols) and p47-CGD clones (white symbols) from three independent differentiations. Diamonds represent monoallelic corrected clones (n = 3-8, mean ± SD, statistics: one-way ANOVA, **** p<0.0001).

Figure 5. DNA methylation analysis of different myeloid promoters in iPSC and iPSC-derived myeloid cells.

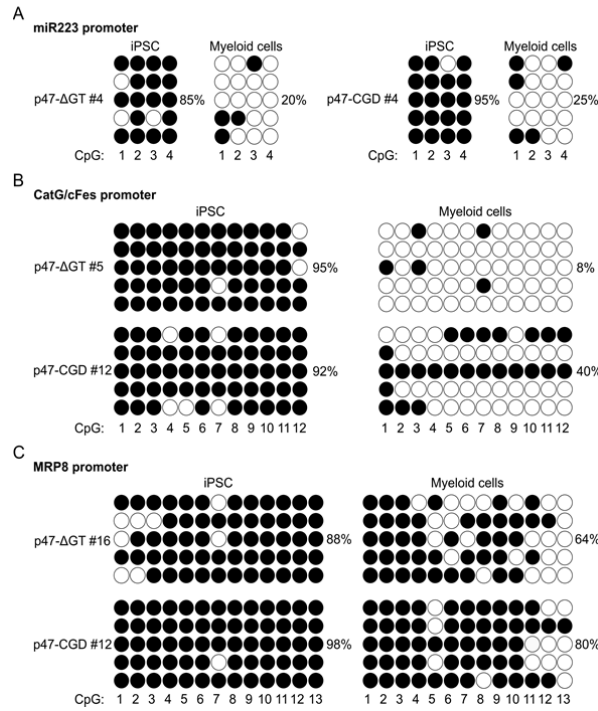


Figure 5. DNA methylation analysis of different myeloid promoters in iPSC and iPSC-derived myeloid cells.

CpG methylation analysis of the miR223 promoter (**A**), CatG/cFes promoter (**B**) and MRP8 promoter (**C**) via bisulfite sequencing in iPSC and iPSC-derived myeloid cells (open circle, non-methylated CpG; filled circle, methylated CpG; mean percentage of CpG methylation are indicated).

Inventory of Supplemental Information

- Figure S1. On-target cleavage activity of the AAVS1-specific sgRNA. Related to Figure 1.
- Figure S2. Analysis of pluripotency marker expression in iPSC after gene correction. Related to Figures 1.
- Supplemental Experimental Procedures
- Supplemental References

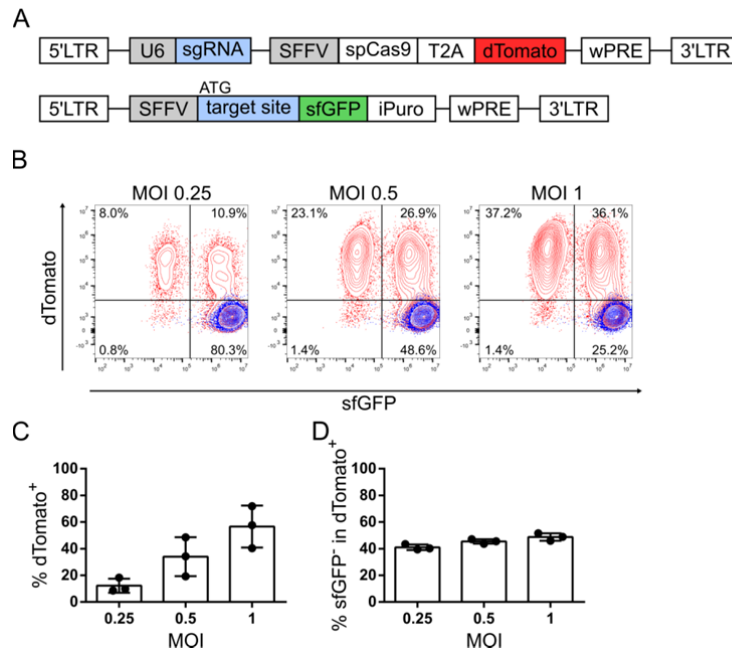


Figure S1. On-target cleavage activity of the AAVS1-specific sgRNA. Related to Figure 1. **(A)** Lentiviral vectors were used to measure the AAVS1-specific sgRNA on-target activity in a HT1080 reporter cell line. Top: All-in-one lentiviral vector applied for CRISPR-Cas9 delivery. Bottom: The lentiviral reporter construct was used to establish the HT1080 reporter cell line. The AAVS1-specific sgRNA target sequence was cloned in frame in front of an sfGFP gene cassette. 5'LTR, 5' long terminal repeat; U6, human U6 promoter; sgRNA, single-guide RNA; SFFV, spleen focus-forming virus promoter; spCas9, *Streptococcus pyogenes*-derived Cas9; T2A, peptide cleavage site; dTomato, a red fluorescent protein; wPRE, woodchuck posttranscriptional regulatory element; 3'LTR, 3' long terminal repeat; sfGFP, super-folder green fluorescent protein; iPuro, internal ribosomal entry site (IRES, abbreviated: i) puromycin resistance gene. **(B)** Representative flow cytometry plots showing loss of sfGFP fluorescence after transduction of HT1080 reporter cells with the CRISPR-Cas9 vector (expressing dTomato) at different MOI (multiplicity of infection). Blue: untransduced HT1080 reporter cells, red: HT1080 reporter cells transduced with CRISPR-Cas9 vector. **(C)** Transduction rate of the CRISPR-Cas9 vector measured as dTomato⁺ cells in the total HT1080 cell population by flow cytometry (n = 3; mean ± SD). **(D)** On-target cleavage activity was quantified as loss of sfGFP fluorescence in HT1080 reporter cells, i.e. as sfGFP⁻ cells in the dTomato⁺ population after transduction of the HT1080 reporter with the CRISPR-Cas9 vector, by flow cytometry (n = 3; mean ± SD).

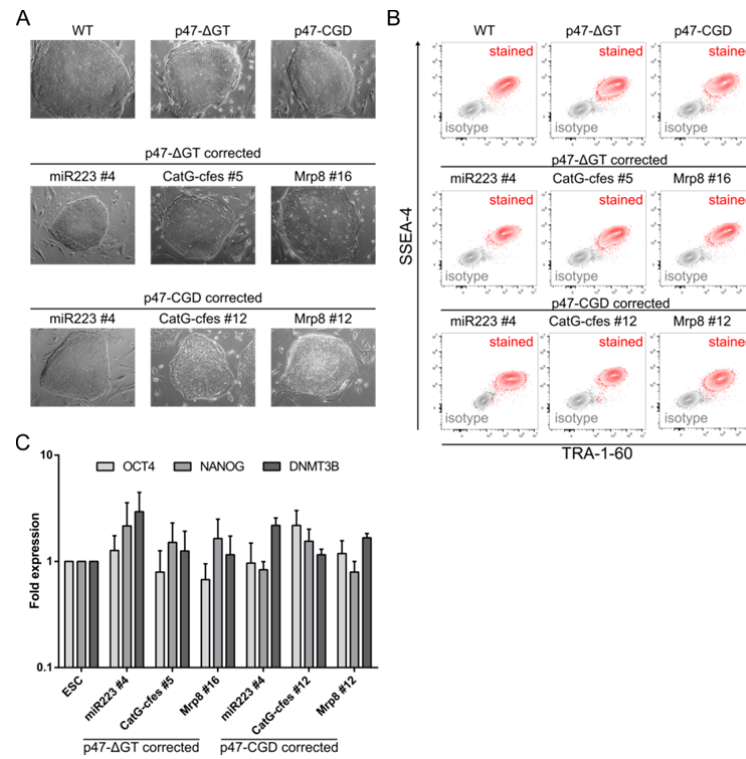


Figure S2. Analysis of pluripotency marker expression in iPSC after gene correction. Related to Figure 1. **(A)** Morphology of iPSC colonies from representative brightfield images. **(B)** Analysis of expression of the pluripotency markers SSEA-4 and TRA-1-60 in viable iPSC by flow cytometry. **(C)** Quantitative PCR analysis measuring mRNA expression levels of the pluripotency markers *OCT4*, *NANOG* and *DNMT3B* in iPSC normalized to β -*ACTIN* and relative to H9 embryonic stem cells (ESC).

Supplemental Experimental Procedures

On-target reporter cell assay

The on-target cleavage activity of the *AAVS1*-specific sgRNA was analyzed in a HT1080 fluorescence reporter assay. The reporter construct (pRRL.PPT.SFFV.target-sfGFP.IRES.Puromycin.wPRE) was cloned by insertion of the 20 nt sgRNA target sequence plus the PAM motif (5'- GTCACCAATCCTGTCCCTAGTGG) in frame with and in front of a super-folder green fluorescent protein (sfGFP) in a lentiviral backbone. To select transduced cells, an IRES.Puromycin cassette was inserted behind the sfGFP. A split packaging system was used to generate viral particles as described before (Maetzig *et al.*, 2014). The reporter cell line was established by transduction of HT1080 cells in the presence of 4 µg/ml protamine sulfate (Sigma Aldrich) with pRRL.PPT.SFFV.target-sfGFP.IRES.Puromycin.wPRE and selection with 5 µg/ml Puromycin. Upon transduction of the HT1080 reporter with the CRISPR-Cas9 vector, sgRNA on-target efficiency was measured by loss of sfGFP fluorescence using flow cytometry (CytoFlex S, Beckman Coulter).

Pluripotency assays

Images of typical iPSC colony morphology were taken at a Zeiss Observer Z1 microscope (AxioVision software). Expression of TRA-1-60 and SSEA-4 was measured by flow cytometry (CytoFlex S). Therefore, single iPSC were blocked with human FcR block (Miltenyi) for 10 minutes and stained with TRA-1-60-DyeLight-488 (clone: TRA-1-60, STEMGENT), SSEA-4-Alexa Fluor 647 (clone: MC813-70, BD) and a PE anti-feeder cell antibody (clone: mEF-SK4, Miltenyi) for 30 min at 4°C. The pluripotency markers *NANOG*, *OCT4* and *DNMT3B* were analyzed via qPCR. Therefore, RNA was isolated using the RNeasy Mini Kit (Qiagen) and reverse transcribed into cDNA using the QuantiTect Reverse Transcription Kit (Qiagen) for each iPSC clone. The qPCR was performed with the Step One Plus Real Time PCR System (Thermo Fisher) and the QuantiTect SYBR Green PCR Kit (Qiagen) according to the manufacturer's instructions in triplicates. The following primers were used: *NANOG* (fw: 5'-TCACACGGAGACTGTCTCTC, rev: 5'-GAACACAGTTCTGGTCTTCTG), *OCT4* (fw: 5'- CCTCACTTCACTGCACTGTA, rev: 5'-CAGGTTTTCTTTCCCTAGCT), *DNMT3B* (fw: 5'- ATAAGTCGAAGGTGCGTCGT, rev: 5'-GGCAACATCTGAAGCCATT) and *β-ACTIN* (fw: 5'- TACCTGTATAGTGTACTTCAT, rev: 5'-

GGTCATGAGAAGTGTTGCTA). The $\Delta\Delta C_t$ method was used to analyze the expression level of all target genes, which were normalized to β -*ACTIN* expression levels and expressed relative to the embryonic stem cell (ESC) clone H9 (Pfaffl, 2001).

Supplementary References

Maetzig, T., Kuehle, J., Schwarzer, A., Turan, S., Rothe, M., Chaturvedi, A., Morgan, M., Ha, T.C., Heuser, M., Hammerschmidt, W. et al. (2014). All-in-One inducible lentiviral vector systems based on drug controlled FLP recombinase. *Biomaterials* 35, 4345-4356.

Pfaffl, M.W. (2001). A new mathematical model for relative quantification in real-time RT-PCR. *Nucleic Acids Res.* 29, 45e–45.